Geophysical Research Letters

RESEARCH LETTER
10.1029/2024GL110129

Could a Low-Frequency Perturbation in the Earth's Magnetotail Be Generated by the Lunar Wake?

K. Nykyri[1], S. Di Matteo[1,2], M. O. Archer[3], X. Ma[4], M. D. Hartinger[5,6], M. Sarantos[1], E. Zesta[1], and W. R. Paterson[1]

[1]NASA Goddard Space Flight Center, Greenbelt, MD, USA, [2]Catholic University of America, Washington, DC, USA, [3]Department of Physics, Imperial College London, London, UK, [4]Center for Space and Atmospheric Research, Embry-Riddle Aeronautical University, Daytona Beach, FL, USA, [5]Space Science Institute, Boulder, CO, USA, [6]University of California Los Angeles, Los Angeles, CA, USA

Key Points:

- A hypothesis for the Earth's magnetic field perturbation caused by the Moon in the magnetotail is proposed
- Magnetometer onboard ARTEMIS spacecraft detects the fundamental frequency corresponding to this theoretical prediction
- These initial findings suggest the need for followup space and ground-based statistical studies of the Moon-Earth field line resonator

Supporting Information:

Supporting Information may be found in the online version of this article.

Correspondence to:

K. Nykyri,
katariina.nykyri@nasa.gov

Citation:

Nykyri, K., Di Matteo, S., Archer, M. O., Ma, X., Hartinger, M. D., Sarantos, M., et al. (2024). Could a low-frequency perturbation in the Earth's magnetotail be generated by the lunar wake? *Geophysical Research Letters*, *51*, e2024GL110129. https://doi.org/10.1029/2024GL110129

Received 3 MAY 2024
Accepted 25 OCT 2024

Abstract Both ground based magnetometers and ionospheric radars at Earth have frequently detected Ultra Low Frequency (ULF) fluctuations at discrete frequencies extending below one mHz-range. Many dayside solar wind drivers have been convincingly demonstrated as driver mechanisms. In this paper we investigate and propose an additional, nightside generation mechanism of a low frequency magnetic field fluctuation. We propose that the Moon may excite a magnetic field perturbation of the order of 1 nT at discrete frequencies when it travels through the Earth's magnetotail ≈4–5 days every month. Our theoretical prediction is supported by a case study of ARTEMIS magnetic field measurements at the lunar orbit in the Earth's magnetotail. ARTEMIS detects statistically significant peaks in magnetic field fluctuation power at frequencies of 0.37–0.47 mHz that are not present in the solar wind.

Plain Language Summary Throughout history, the Moon has both captivated the human mind as well as had important practical consequences on the lives of people in coastal areas. Humans have attributed the Full Moon to all types of things, many of which do not stand up to scientific scrutiny. Recent spacecraft measurements have shown that the Moon has significant magnetic anomalies that are strong enough for producing a magnetic cavity in the solar wind plasma. The Moon also has a wake structure with a strong electrostatic potential which may act as a perturbation for the magnetic field lines. Here, by using ARTEMIS spacecraft observations in the magnetotail, we found surprisingly that the Moon may weakly perturb the Earth's magnetosphere when it travels through the magnetotail in about 4–5 days around the time of the Full Moon. This effect may have been stronger in the past, when Moon was closer to the Earth and its magnetic field was stronger.

1. Introduction

Both ground based magnetometers and ionospheric radars at Earth have frequently detected Ultra Low Frequency (ULF) fluctuations at discrete frequencies (Samson, Harrold, et al., 1992; Samson, Wallis, et al., 1992). While it has been reported that there may be quasi-steady preferential frequencies (≈0.65, 1.3, 1.9, 2.6, 3.3, and 4.8 mHz) of such discrete pulsations (Chisham & Orr, 1997; Fenrich et al., 1995; Francia & Villante, 1997; Villante et al., 2001), other statistical studies have instead reported little evidence of predominant frequencies standing out from a continuum (Baker et al., 2003; Rae et al., 2012). Nonetheless, numerous possible sources of discrete frequency ULF waves have been considered:

1. Magnetospheric cavity/waveguide modes between the magnetopause and a turning point (Chen & Kivelson, 1991; Hartinger et al., 2012; Samson, Harrold, et al., 1992; Samson, Wallis, et al., 1992)
2. Solar wind density fluctuations whose changes in solar wind dynamic pressure drive the magnetosphere globally in a "forced breathing" mode (Di Matteo et al., 2022; Kepko et al., 2002; Viall et al., 2009)
3. Standing wave eigenmodes of the dayside magnetopause surface (Archer & Plaschke, 2015; Chen & Hasegawa, 1974; Plaschke et al., 2009), triggered by impulsive upstream drivers such as magnetosheath jets (Archer et al., 2013, 2019).

In this paper we investigate a possible additional nightside generation mechanism of low amplitude magnetic field fluctuations around the lowest reported discrete frequency ULF wave below 1 mHz. We propose, using

ARTEMIS data and numerical simulations, that the Moon may excite weak magnetic field perturbations when it travels through the Earth's magnetotail ≈4–5 days every month, resulting in long-period Alfvén waves.

When the solar wind encounters Earth's magnetic field it stretches the Earth's (mostly dipolar) magnetosphere into an elongated structure, called the magnetotail. The magnetotail divides into two lobes; field lines in the northern lobe point generally toward the Earth, and field lines in the southern lobe point away from the Earth. Because the magnetic fields point into opposite directions, according to Ampere's law there exists a cross-tail current. The plasma sheet, which contains this cross-tail current, has denser plasma than the lobes and has a very weak magnetic field.

In Geocentric Solar Magnetospheric (GSM) coordinates, the x-axis points from Earth to Sun, y-axis is perpendicular to the x, z-plane, which contains the Earth's magnetic dipole. As the Earth rotates around its axis once in 24 hr, the dipole axis (which is not aligned with the rotation axis) takes turns pointing toward the Sun and away from the Sun. This wobble of the geo-dipole is primarily due to this diurnal motion and makes the Earth's magnetotail to move up and down in the z-direction.

The Moon enters the magnetotail at about $x \approx -60\ R_E$ from Earth every month, ≈2–3 days before the full Moon, and traverses through it in ≈4–6 days. The diurnal wobble of the geodipole makes the Moon cross both the northern and southern lobe magnetic field lines. Besides this motion, the magnetotail current sheet is prone to various instabilities, for example, kink and sausage modes, which produce fluctuations at higher frequencies (than the diurnal wobbling of the geodipole) at ≈10–80 mHz (≈13–100 s) and ≈50–130 mHz (≈8–20 s), respectively (Smith et al., 1997). The presence of these higher frequency wave modes would also increase the Moon's encounters with the lobe field lines of different polarity. Seasonal effects may also arise due to the tilt of the Moon's orbit relative to ecliptic plane and due to the dipole tilt direction lifting the current sheet above and below the ecliptic.

2. A Hypothesis for the Moon Generated Magnetic Perturbation

It may sound surprising to consider that the Moon could perturb Earth's magnetic field lines when it is in the magnetotail, as the Moon has been generally thought as an insulator. However, when embedded in the fast plasma flow, such as solar wind, a wake-like structure with complex plasma dynamics and properties has been observed behind the Moon (e.g., Colburn et al., 1967; Ness et al., 1967; Spreiter et al., 1970; Whang, 1970). Recent observations by the two-spacecraft Acceleration, Reconnection, Turbulence and Electrodynamics of the Moon's Interaction with the Sun (ARTEMIS) mission (Angelopoulos, 2011) show that the lunar wake can extend 12 lunar radii (R_L) behind the Moon, corresponding to about 3.3 R_E (Zhang et al., 2014). In addition, it has been recently shown that the Moon has magnetic anomalies which are capable of producing a mini-magnetosphere when the Moon is embedded in the solar wind flow (Wieser et al., 2010).

When the Moon is in the magnetotail it can be frequently bombarded by plasmoids and bursty bulk flows (BBFs) that result from magnetospheric substorm and tail reconnection dynamics (Angelopoulos et al., 2008). The typical waiting time between substorms is about 2–4 hr (Borovsky & Yakymenko, 2017). Assuming each substorm results in a plasmoid, the Moon could be bombarded 6 to 12 times a day by higher density plasma each day it spends in the magnetotail. Indeed, two ARTEMIS spacecraft have observed a tailward moving plasmoids at lunar orbit (Li et al., 2013; Nykyri et al., 2019). Periodic (∼1.7 mHz) flow oscillations, likely driven by BBFs or Kelvin-Helmholtz waves have also been frequently observed in the magnetotail (De Spiegeleer et al., 2017) which may also periodically impact the charged particle environment around the Moon.

The brightness of the lunar sodium exosphere is correlated with the Moon's passage through the Earth's magnetotail plasma sheet (Wilson et al., 2006), where the plasma ions impact the source rates of the lunar exosphere (Sarantos et al., 2008). Results from Lunar Prospector data suggest that in the plasma sheet surface charging can result in −600 V electrostatic potential in the night-side of the Moon (Stubbs et al., 2007). It is therefore plausible, that when exposed to the plasma sheet, the lunar surface can charge up resulting in some net surface charge density. We propose that the extended lunar wake, magnetic anomaly and net surface charge density combined with the magnetospheric dynamics and diurnal flapping motion (see Figure 1) of the magnetotail about the charged Moon may generate a low-frequency magnetic field oscillation on these field lines. Figure 1 shows an illustration of the different phases (panels a–c) of the diurnal wobble of geodipole modeled after Tsyganenko 96 model (Tsyganenko, 1996) in $x - z$ -plane in GSM coordinates. The magnetic perturbation along z-direction is

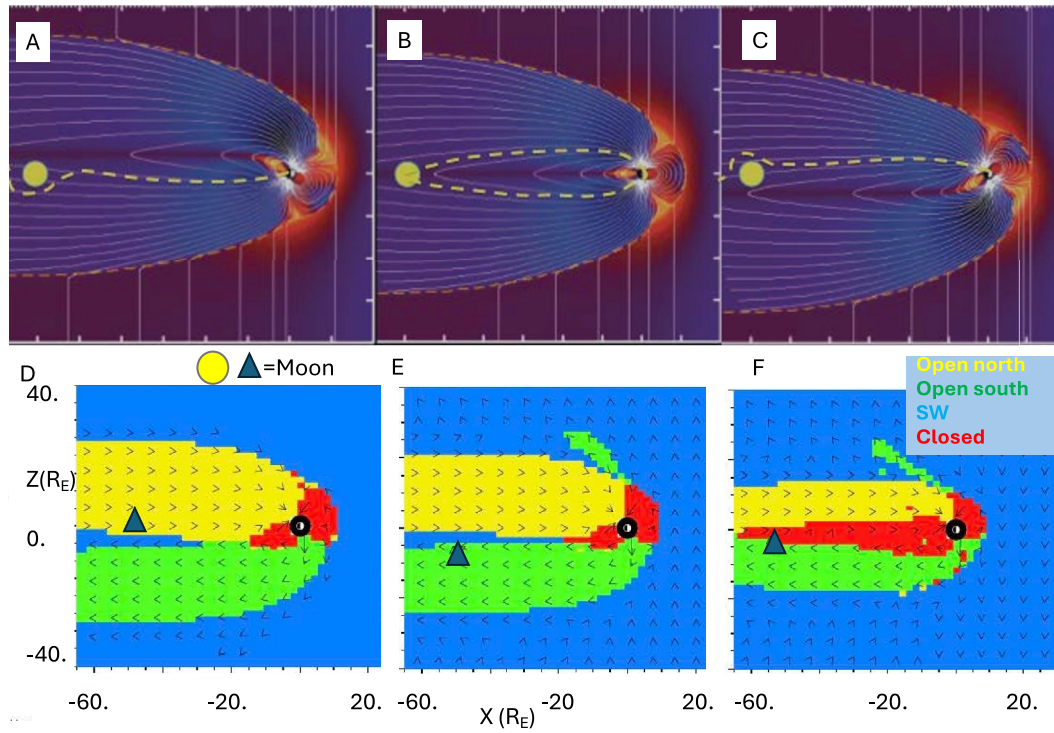

Figure 1. Top row shows an illustration of Moon produced perturbations during different phases of the diurnal wobble of the geodipole (a–c). The magnetic field lines are modeled after the Tsyganenko 96 model (Tsyganenko, 1996). The Moon's mini-magnetosphere is depicted with a yellow circle at $x = -60\ R_E$. This Figure is adapted from the animation generated by Tsyganenko at http://geo.phys.spbu.ru/tsyganenko/modeling.html. Bottom row shows the location of the Moon and two ARTEMIS spacecraft (triangles) in the global simulation in x, z_{GSM}-plane with magnetic field topology color coded at different times of the simulation. The arrows show the direction of the local magnetic field. At 02:24 UT on 12/31/2017 (d), 2 days before the full Moon on 01/02/2018, the Moon (projected into $y = 0$-plane) is on field lines where the other end connects to solar wind and the other end connects to Northern hemisphere of the Earth (marked with yellow topology). Panels (e and f) illustrate how the Moon encounters both open (green) and closed (red) field line topologies during its traversal through the magnetotail.

illustrated. A similar perturbation can be created along y-direction due to the Moon's motion relative to Earth's magnetic field. We expect this effect to be stronger when the Moon encounters the plasma sheet more frequently.

Wave behavior on a vibrating string can be expressed in terms of the wave equation, which in 1-D can be written as:

$$\frac{\partial^2 \Psi(x,t)}{\partial x^2} - \frac{1}{v^2}\frac{\partial^2 \Psi(x,t)}{\partial t^2} = 0 \tag{1}$$

where, $v = \sqrt{\frac{T}{m/L}}$ is the wave phase speed which is a function of tension, T, and mass per unit length of the string, m/L.

Here, we perform simple back-of-the-envelope, 1-D, calculations (similar to Sugiura and Wilson (1964)) to evaluate the approximate frequency range of these field line resonance (FLR) frequencies in the Earth's magnetotail. Now, the phase speed becomes the Alfvén speed, $v_A = B/\sqrt{\mu_0 \rho}$, where B is the magnetic field strength, and ρ is the mass density on the particular magnetic field line (both assumed constant here). Typical range of v_A in the magnetotail varies between few hundreds to few thousands of km/s, depending on the solar wind conditions, how compressed the tail is and whether in the plasma sheet, tail lobes, or in the lunar wake. Assuming a typical string length, L, the fixed-end solution, with foot points in both ionospheres, becomes

$$\Psi(x,t)_n = A_n \sin(n\pi x/L) e^{i\left[(n\pi v_A t/L)+\phi_n\right]} \tag{2}$$

with $\lambda_n = 2L/n$ and eigenfrequencies of $f_n = v_A/\lambda_n = nv_A/2L$, where n =1, 2, 3, …, and where $n = 1$ corresponds to the fundamental frequency.

The mixed boundary conditions, with one fixed end at the ionosphere and one open end into the solar wind, give wavelengths $\lambda_m = 4L_m/m$ yielding eigenfrequencies of $f_m = mv_A/4L_m$, where m is an odd-integer, that is, m = 1,3,5,…

A single harmonic frequency can be excited on a guitar string, if the shape of the string is perturbed into a shape of the standing wave of one of the harmonics. An entire spectrum of harmonic frequencies can be generated if the string is being tucked or pulled and then released. Due to the Moon's motion through the magnetotail, the Moon could potentially act as the harmonic generator at a distance $x = R_M$ from the Earth and it will encounter both closed and open geomagnetic field lines, corresponding to field line lengths of $L = 2 \times R_M$ and $L_M = R_M$, for fixed-end and mixed boundary conditions, respectively. When it encounters stretched, closed field lines, the perturbation travels to the northern and southern ionosphere, and gets reflected, forming a standing wave. The magnetic field lines that originate from higher latitudes, have longer length, and those closest to the plasma sheet are the shortest.

For example, setting the field line length to $L = 2 \times 60\ R_E = 120\ R_E$ and choosing, (a) $v_A = 600$ km/s would give $f_n = 0.392$, 0.785, 1.177 mHz for $n = [1, 2, 3]$, respectively. If the solar wind speed doubles, or the density increases by factor of 4, the dynamic pressure increases by factor of 4 and the magnetotail becomes more compressed, so Alfvén speed on the field lines encountered by the Moon at higher z-coordinate is larger, but also the field line length increases. For example, using v_A = (b) 1,000 km/s and $L = 3 \times 60R_E$, would give $f_n = 0.436$, 0.872, 1.308 mHz. The mixed boundary condition with $L_m = 60\ R_E$, yields $f_m = 0.436$, 1.308, 2.18 mHz, for $n = [1,3,5]$, respectively. In addition, the distance from Earth to the Moon is not constant. The extreme values for the Moon distance to the Earth, when it travels through the magnetotail, can occur when the Moon is close to perigee or apogee passage. These values typically range from 56 R_E to 63.5 R_E.

The $n > 1$ values estimated above are in the range of the reported discrete frequency ULF waves but these could be generated by multiple sources. The original discovery of discrete frequencies at 1.3, 1.9, 2.6–2.7, and 3.2–3.4 mHz in the power spectrum of Doppler velocities of the HF radar were observed from local midnight to morning sector (Samson et al., 1991). Five out of six events occurred within 5 days from the Full Moon. While these frequencies were attributed to waveguide modes, this has been questioned due to the field line lengths and densities required to match the observations (Allan & McDiarmid, 1993; Archer et al., 2015; Harrold & Samson, 1992; Mann et al., 1999). At 69 degrees of latitude, most power occurred at 1.9 mHz, although the 1.3 mHz peak and even lower frequency peaks at ≈0.65 mHz and ≈0.3 mHz were visible. While multiple sources could potentially create the higher, >1 mHz, frequencies (e.g., cavity modes or large-wavelength KH waves), the fundamental frequencies <0.8 mHz would be difficult to reconcile with a cavity mode for the typically observed values of solar wind dynamic pressure. For example, dayside FLRs with frequencies ∼ 0.8 mHz have been reported (Mathie & Mann, 2000) for solar wind dynamic pressure of 0.2–0.5 nPa (about 4–5 times smaller than for the present event), which would place the magnetosphere in an abnormally expanded state.

3. MHD Simulations of Magnetotail Dynamics

To demonstrate that the values we have chosen for the typical Alfvén speeds and field line lengths above are appropriate, we modeled the "super Full Moon" event of 01/02/2018 with BATSRUS global MHD simulation (Run Katariina_Nykyri_031318_1) in Community Coordinated Modeling Center (CCMC) (Tóth et al., 2005). While the MHD simulations do not capture the self-consistent interaction with the Moon, they can be used for studying the motion of the virtual Moon through the magnetotail. Figures 1d–1f shows the location of the Moon and two ARTEMIS spacecraft (triangles) in the global simulation in x, z_{GSM}-plane with magnetic field topology color coded at different times of the simulation. The arrows show the direction of the local magnetic field. At 02:24 UT on 12/31/2017 (panel d), 2 days before the full Moon on 01/02/2018, the Moon (projected into $y = 0$-plane) is on field lines where one end connects to solar wind and the other end connects to Northern hemisphere of the Earth (marked with yellow topology). The panels d–f illustrate how the Moon encounters both open and closed field line topologies during its traversal through the magnetotail, corresponding to mixed and fixed-end solutions, respectively. Figures S1 and S2 in Supporting Information S1 show the ARTEMIS (THB) plasma,

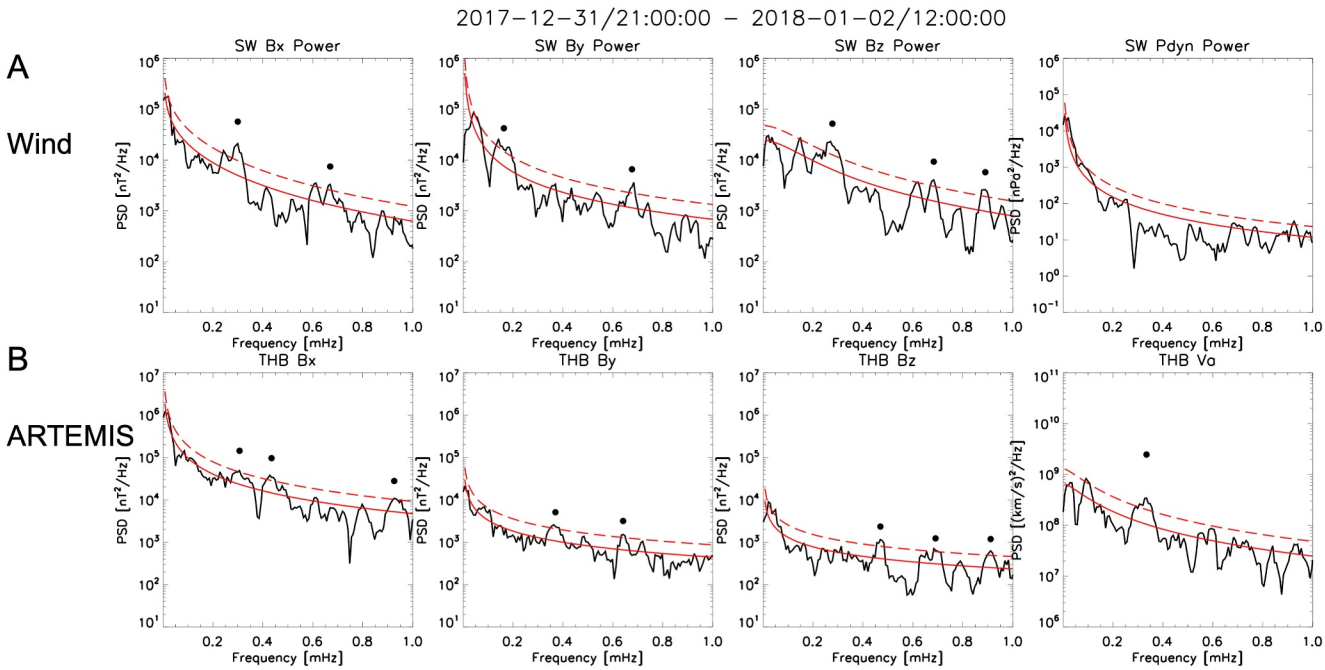

C Frequency in mHz. Detection at the 95% confidence level with uncertainty of $\Delta f = \pm 0.04$ mHz.

Wind Bx		**0.30**		0.67		
Wind By	0.16			**0.68**		
Wind Bz		0.28		**0.68**		**0.89**
Wind Pdyn						
ARTEMIS Bx		**0.31**	0.43			0.93
ARTEMIS By			0.37	**0.64**		
ARTEMIS Bz			0.47	**0.69**		**0.91**
ARTEMIS Va		0.33				

Bold values: Same frequency observed at Wind and THEMIS

Red values: Frequency observed only at ARTEMIS

Figure 2. Power of fluctuations of magnetic field components (in GSM coordinates) as a function of frequency between 31 December 2017, at 21:00 UT and 2 January 2018, at 12:00 from Wind (shifted in time of ≈50 min) at top row (a) and from ARTEMIS (THEMIS-B = THB) at the bottom row (b). In addition the power of flow pressure fluctuations in the solar wind and the Alfvén speed fluctuations as measured by ARTEMIS in the magnetotail are shown. Panel c compares statistically significant peaks at each component marked by black dots in panel (a) and (b). Bold values indicate the peaks that are observed both at Wind and ARTEMIS and red values the ones detected only at ARTEMIS.

field and Alfvén-speed measurements during 12/31/2017/21:00–1/2/2018/12:00, and Alfvén speed between 12/30/2017/00:00 and 1/4/2018/00:00 measured by virtual spacecraft in the MHD simulation and by the ARTEMIS.

The mean measured v_A by ARTEMIS (THB) during 12/31/2017/21:00–1/2/2018/12:00 is 626 km/s and the average distance from the Moon to Earth is 55.6 R_E. Both for the fixed-end and mixed boundary conditions, this average value of v_A and the field line length of $L = [2 \times 55.6, 55.6]$ R_E would yield the fundamental mode frequencies of 0.44 mHz, respectively. We also performed ray tracing calculations in the MHD simulations (see Table S2 in Supporting Information S1) to evaluate the relative impact of the Alfvén speed variation along the field line on the FLR frequencies.

4. ARTEMIS (THB) and Wind Power Spectral Density (PSD) Observations

Figure 2 presents power of fluctuations of magnetic field components (in GSM coordinates) as a function of frequency between 12/31/2017/21:00 and 1/2/2018/12:00 from Wind spacecraft (shifted of ≈50 min) at top row

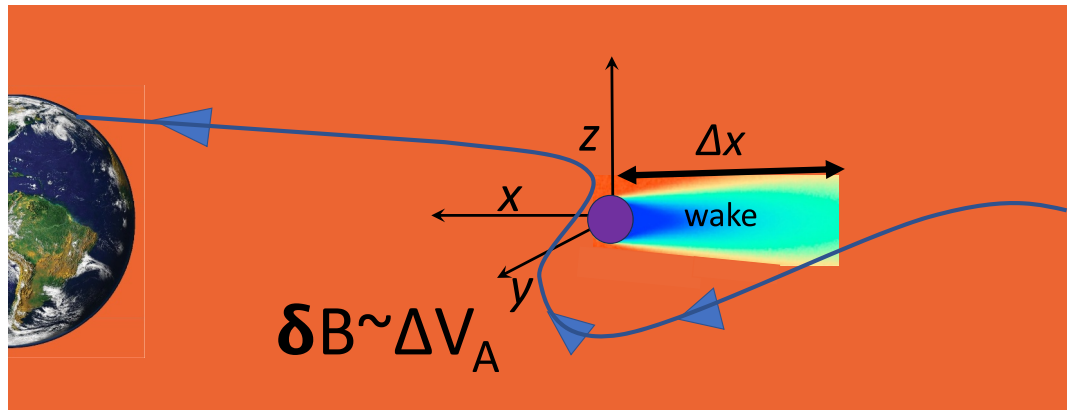

Figure 3. A schematic showing how the relative motion of the Earth's magnetic field about the lunar wake, could create a magnetic field perturbation, $\delta\mathbf{B}$, proportional to the change of the Alfvén speed. The length of the lunar wake is denoted as Δx. The lunar wake is taken into the figure and adapted from simulations by Gharaee et al. (2015).

(a) and from ARTEMIS at the bottom row (b) up to 1 mHz. In addition, the power of flow pressure fluctuations in the solar wind and the Alfvén speed fluctuations as measured by ARTEMIS in the magnetotail are shown. We use the spectral analysis approach of Di Matteo et al. (2021) in which a bending power law function is fitted to the power spectral density (PSD) to identify the power background level (red line in Figures 2a and 2b). Peaks in the PSD are considered significant when above the 95% confidence threshold (red dashed line in Figures 2a and 2b). The ≈0.3 mHz, ≈0.64–0.69 mHz, ≈0.89–0.93 mHz peaks are present both at Wind and ARTEMIS data so these may be driven by IMF fluctuations. However, the statistically significant peaks at 0.43, 0.37, and 0.47 mHz for the B_x, B_y and B_z fluctuation power, respectively, are only detected by ARTEMIS and are very close to the theoretically predicted fundamental frequency of 0.44 mHz. The maximum PSD of 3.4×10^4 nT^2/Hz is detected at 0.43 mHz in B_x-fluctuations corresponding to a perturbation amplitude of 1.24 nT in the B_x component. The PSD reached values of at 2.4×10^3 nT^2/Hz at 0.37 mHz in B_y-fluctuations, and 1.2×10^3 nT^2/Hz at 0.47 mHz in B_z-fluctuations. These values correspond to perturbation amplitude of ≈0.33 nT and ≈0.21 nT, respectively.

Figure S3 in Supporting Information S1 shows that the 0.47 and 0.33 mHz PSD peaks in B_z and V_A measured by THB remain even at the 99% confidence level, while these are absent in the Wind measurements. The spectral analysis (see Figure S4 in Supporting Information S1) of the magnetic field components and Alfvén speed in the MHD simulation along the virtual Moon, THB and THC reveal no significant peaks at these frequencies. This suggests there are no intrinsic global magnetospheric modes at these frequencies during this event.

The IMF or solar wind flow pressure fluctuations likely are not the direct cause of these (0.37–0.47 mHz) frequencies since no significant peak occur in the corresponding PSD at Wind (see Figure 2) or at ACE (see Figure S5 in Supporting Information S1). We also performed (see Figure S6 in Supporting Information S1) the same PSD analysis shown in Figure 2 but using shorter 12 hr intervals (with a 30 min shift and 95% confidence level) which revealed the same, statistically significant peaks in PSDs of B_x and B_y, which were not present in the solar wind.

5. Discussion and Conclusions

Figure 3 depicts how the Moon and the motion of the Lunar wake relative to the Earth's magnetotail could generate a low frequency fluctuation on the Earth's magnetic field lines.

To estimate the magnetic field perturbation, δB, the Moon produces on magnetotail field lines with strength of B_0, we consider the change in the Alfvén speed, ΔV_A, produced by the motion of the lunar wake relative to background magnetic field as follows,

$$\delta B/B_0 = \Delta V_A/V_{A,0} \tag{3}$$

The magnitude of the change in the Alfvén speed between the wake and the background can be calculated as,

$$\Delta V_A = |V_{A,wake} - V_{A,0}| \tag{4}$$

$$= |\frac{B_{wake}}{\sqrt{\mu_0 m_p n_{wake}}} - \frac{B_0}{\sqrt{\mu_0 m_p n_0}}| \tag{5}$$

where m_p is the proton mass, and B_{wake} and n_{wake} are the magnetic field strength and plasma number density in the lunar wake, respectively.

Using ARTEMIS measurements after the spacecraft transit through the lunar wake (see Figure S1 and Table S1 in Supporting Information S1), we get δB =0.99 nT, for taking $B_0 = 7.68$ nT, $n_0 = 0.05/cc$, $B_{wake} = 7.82$ nT, $n_{wake} = 0.07/cc$. With measurement before the spacecraft transit through the lunar wake, we obtained δB =3.65 nT, for taking the same value for the lunar wake and ambient values of $B_0 = 12.5$ nT and $n_0 = 0.09/cc$. The overall range of the estimated magnetic field perturbation, $\delta B = 0.99 - 3.65$ nT is consistent with the wave amplitude range we obtained from the spectral analysis of the magnetic field at ARTEMIS, that is 0.21–1.24 nT.

An alternative approach to estimate the magnetic field perturbation is considering the lunar plasma interaction with the environment of the terrestrial magnetotail. While the formation of a plasma wake during the moon interaction with solar wind plasma has been largely discussed, the existence of a plasma wake in the magnetotail environment has been only recently reported (Liuzzo et al., 2021). In the magnetotail, the lunar ionosphere often exceeds by over an order of magnitude the local plasma density (Harada et al., 2013; Poppe et al., 2012; Tanaka et al., 2009), therefore playing a significant role in the exchange of mass and momentum with the magnetospheric plasma and in the perturbation of the magnetospheric electromagnetic fields (Cao et al., 2020). Liuzzo et al. (2021) have also reported a case study in which alignment of the magnetic field and plasma flow made both lunar and magnetospheric ions unable to access the lunar wake. In this situation the pressure balance is maintained by the magnetic field only. We follow a similar approach of Liuzzo et al. (2021), who used the Simon et al. (2012) method for complete evacuation of plasma in the lunar wake, that gives:

$$\delta B = B_0\left(\sqrt{\beta_0 + 1} - 1\right) \tag{6}$$

where β_0 is the ambient plasma β. Using the time intervals before and after the ARTEMIS lunar wake transit, we obtained δB =2.16 nT for taking $\beta_0 = 0.38$ before the wake transit and δB =0.40 nT for taking $\beta_0 = 0.24$ after the wake transit. The perturbation amplitudes are consistent with our previous estimates and measurements.

In this letter we have proposed a hypothesis for the generation of low frequency magnetic field fluctuations in the lowest range of the magnetospheric discrete frequency ULF waves by the perturbation produced by the lunar wake when it travels through the Earth's magnetotail. These preliminary results, based on classical wave theory, ARTEMIS observations and MHD simulations, suggest that close to the lunar orbit, the Moon may produce these ≈1 nT amplitude, very low frequency magnetic field fluctuations at the frequency range of 0.37–0.47 mHz. The Geotail spacecraft, which was located at the dusk sector, closer to Earth at ($\mathbf{R}_{GSE} = [-11, 24, 10]\ R_E$), did observe the same ∼0.3 mHz peak that was present in the solar wind and at THB. However, it did not detect the 0.4–0.5 mHz peak seen at THB near the Moon, suggesting that the ∼1 nT perturbation produced by the Moon is rather localized in L-shell and MLT. The amplitude and frequency range of these fluctuations is consistent with some of the ISEE-2 measurements of ULF waves in the tail lobe closer to Earth (Chen & Kivelson, 1991). Future work should try map along the field line and measure these potentially Moon-produced peaks at the same MLT closer to Earth. As the magnetic field is stronger closer to the Earth, the parallel gradient in the Alfvén speed may lead to a strong wave reflection if the parallel wave length of Moon-induced Alfvén wave is longer than the Alfvén speed gradient scale. This could lead to a standing wave at a discrete driving frequency. To identify the properties of a possible standing wave would require multi-spacecraft measurement along the field line. This type analysis could be properly targeted by current multi spacecraft mission concept in the magnetosphere (e.g., Kepko et al., 2022; Retinò et al., 2022).

One lunar precession takes about 18.6 years which affects the ecliptic latitude at which the Moon crosses the magnetotail and thus the number and duration of lunar encounters with the plasmasheet (Hapgood, 2007). Modeling results suggest that for the period of 1960–2030, the total lunar exposure to the plasmasheet will vary

from 10 hr per month at a minimum to 40 hr per month at the maximum (Hapgood, 2007). Therefore, it is plausible that the lunar surface charging, and therefore the strength of the magnetic perturbation, will differ between different times during the near 18-year cycle. This could be tested in future statistical studies using both space-based and ground based magnetometers. Currently, 14+ years of ARTEMIS data exists at lunar orbit which could be used to study the PSDs at the different fundamental frequencies and their dependence on upstream solar wind and IMF conditions. These initial findings also highlight the need to develop numerical simulations that self-consistently take into account lunar wake effects in the Earth's magnetosphere.

Finally, as the Moon had a stronger magnetic field and was closer to the Earth in the past, it is interesting to consider how strong the magnetic field perturbation produced by the Moon may have been. As the NASA sends the first woman and the next man to the surface of the Moon in 2026, it would be useful to install Moon-based magnetometers at different locations on the Moon and also bring back more rock samples collected at various depths and locations on the Moon. This would help uncover the magnetic history of the Moon and its past impact on the Earth's magnetic field.

Data Availability Statement

The present study has utilized ARTEMIS spacecraft data and SPEDAS software (Angelopoulos et al., 2019) which are freely available from https://spedas.org/wiki/. Magnetic field data is from the flux gate magnetometer (Auster et al., 2008) and plasma measurements are from the electrostatic analyzer (McFadden et al., 2008). Interplanetary magnetic field data is from the Magnetic Field Investigation (Lepping et al., 1995) and solar wind plasma data is from the Solar Wind Experiment (Ogilvie et al., 1995) onboard the Wind spacecraft. This work was carried out using the SWMF/BATSRUS tools developed at the U. of Michigan Center for Space Environment Modeling (CSEM) and made available through the NASA CCMC at GSFC through their public Runs on Request system (http://ccmc.gsfc.nasa.gov). The specific Run number is Katariina_Nykyri_031318_1. The data sets for this research are available in this in-text data citation reference (Nykyri, 2024) with the creative commons license CCBY4.0.

Acknowledgments
Work by KN and XM was supported by NASA Grant 80NSSC23K0899. SD was supported by NASA Grant 80NSSC21K0459. MA is supported by a UKRI (STFC/EPSRC) Stephen Hawking Fellowship EP/T01735X/1. MH was supported by NSF Grants AGS-2027210 and AGS-2307204. In addition work by KN, SD, MA, and MH were supported by the International Space Science Institute (ISSI) in Bern, through ISSI International Team project 546 "Magnetohydrodynamic Surface Waves at Earth's Magnetosphere (and Beyond)."

References

Allan, W., & McDiarmid, D. R. (1993). Frequency ratios and resonance positions for magnetospheric cavity/waveguide modes. *Annales Geophysicae*, *11*, 916–924.

Angelopoulos, V. (2011). The ARTEMIS mission. *Space Science Reviews*, *165*(1–4), 3–25. https://doi.org/10.1007/s11214-010-9687-2

Angelopoulos, V., Cruce, P., Drozdov, A., Grimes, E. W., Hatzigeorgiu, N., King, D. A., et al. (2019). The space physics environment data analysis system (SPEDAS). *Space Science Reviews*, *215*(1), 9. https://doi.org/10.1007/s11214-018-0576-4

Angelopoulos, V., McFadden, J. P., Larson, D., Carlson, C. W., Mende, S. B., Frey, H., et al. (2008). Tail reconnection triggering substorm onset. *Science*, *321*(5891), 931–935. https://doi.org/10.1126/science.1160495

Archer, M. O., Hartinger, M. D., & Horbury, T. S. (2013). Magnetospheric "magic" frequencies as magnetopause surface eigenmodes. *Geophysical Research Letters*, *40*(19), 5003–5008. https://doi.org/10.1002/grl.50979

Archer, M. O., Hartinger, M. D., Walsh, B. M., Plaschke, F., & Angelopoulos, V. (2015). Frequency variability of standing Alfvén waves excited by fast mode resonances in the outer magnetosphere. *Geophysical Research Letters*, *42*(23), 10150–10159. https://doi.org/10.1002/2015GL066683

Archer, M. O., Hietala, H., Hartinger, M. D., Plaschke, F., & Angelopoulos, V. (2019). Direct observations of a surface eigenmode of the dayside magnetopause. *Nature Communications*, *10*(1), 615. https://doi.org/10.1038/s41467-018-08134-5

Archer, M. O., & Plaschke, F. (2015). What frequencies of standing surface waves can the subsolar magnetopause support? *Journal of Geophysical Research: Space Physics*, *120*(5), 3632–3646. https://doi.org/10.1002/2014JA020545

Auster, H. U., Glassmeier, K. H., Magnes, W., Aydogar, O., Baumjohann, W., Constantinescu, D., et al. (2008). The THEMIS fluxgate magnetometer. *Space Science Reviews*, *141*(1–4), 235–264. https://doi.org/10.1007/s11214-008-9365-9

Baker, G. J., Donovan, E. F., & Jackel, B. J. (2003). A comprehensive survey of auroral latitude Pc5 pulsation characteristics. *Journal of Geophysical Research*, *108*(A10), SMP11-1. https://doi.org/10.1029/2002JA009801

Borovsky, J. E., & Yakymenko, K. (2017). Substorm occurrence rates, substorm recurrence times, and solar wind structure. *Journal of Geophysical Research: Space Physics*, *122*(3), 2973–2998. https://doi.org/10.1002/2016JA023625

Cao, X., Halekas, J., Poppe, A., Chu, F., & Glassmeier, K.-H. (2020). The acceleration of lunar ions by magnetic forces in the terrestrial magnetotail lobes. *Journal of Geophysical Research: Space Physics*, *125*(6), e27829. https://doi.org/10.1029/2020JA027829

Chen, L., & Hasegawa, A. (1974). A theory of long-period magnetic pulsations: 2. Impulse excitation of surface eigenmode. *Journal of Geophysical Research*, *79*(7), 1033–1037. https://doi.org/10.1029/JA079i007p01033

Chen, S.-H., & Kivelson, M. G. (1991). On ultralow frequency waves in the lobes of the Earth's magnetotail. *Journal of Geophysical Research*, *96*(A9), 15711–15724. https://doi.org/10.1029/91JA01422

Chisham, G., & Orr, D. (1997). A statistical study of the local time asymmetry of Pc 5 ULF wave characteristics observed at midlatitudes by SAMNET. *Journal of Geophysical Research*, *102*(A11), 24339–24350. https://doi.org/10.1029/97JA01801

Colburn, D. S., Currie, R. G., Mihalov, J. D., & Sonett, C. P. (1967). Diamagnetic solar-wind cavity discovered behind Moon. *Science*, *158*(3804), 1040–1042. https://doi.org/10.1126/science.158.3804.1040

De Spiegeleer, A., Hamrin, M., Pitkänen, T., Volwerk, M., Mann, I., Nilsson, H., et al. (2017). Low-frequency oscillatory flow signatures and high-speed flows in the Earth's magnetotail. *Journal of Geophysical Research: Space Physics*, *122*(7), 7042–7056. https://doi.org/10.1002/2017JA024076

Di Matteo, S., Viall, N. M., & Kepko, L. (2021). Power spectral density background estimate and signal detection via the multitaper method. *Journal of Geophysical Research: Space Physics*, *126*(2), e2020JA028748. https://doi.org/10.1029/2020ja028748

Di Matteo, S., Villante, U., Viall, N., Kepko, L., & Wallace, S. (2022). On differentiating multiple types of ULF magnetospheric waves in response to solar wind periodic density structures. *Journal of Geophysical Research: Space Physics*, *127*(3), e2021JA030144. https://doi.org/10.1029/2021ja030144

Fenrich, F. R., Samson, J. C., Sofko, G., & Greenwald, R. A. (1995). ULF high- and low-m field line resonances observed with the super dual auroral radar network. *Journal of Geophysical Research*, *100*(A11), 21535–21547. https://doi.org/10.1029/95JA02024

Francia, P., & Villante, U. (1997). Some evidence of ground power enhancements at frequencies of global magnetospheric modes at low latitude. *Annales Geophysicae*, *15*(1), 17–23. https://doi.org/10.1007/s00585-997-0017-2

Gharaee, H., Rankin, R., Marchand, R., & Paral, J. (2015). Properties of the lunar wake predicted by analytic models and hybrid-kinetic simulations. *Journal of Geophysical Research: Space Physics*, *120*(5), 3795–3803. https://doi.org/10.1002/2014JA020907

Hapgood, M. (2007). Modelling long-term trends in lunar exposure to the Earth's plasmasheet. *Annales Geophysicae*, *25*(9), 2037–2044. https://doi.org/10.5194/angeo-25-2037-2007

Harada, Y., Machida, S., Halekas, J. S., Poppe, A. R., & McFadden, J. P. (2013). ARTEMIS observations of lunar dayside plasma in the terrestrial magnetotail lobe. *Journal of Geophysical Research: Space Physics*, *118*(6), 3042–3054. https://doi.org/10.1002/jgra.50296

Harrold, B. G., & Samson, J. C. (1992). Standing ULF modes of the magnetosphere: A theory. *Geophysical Research Letters*, *19*(18), 1811–1814. https://doi.org/10.1029/92GL01802

Hartinger, M. D., Angelopoulos, V., Moldwin, M. B., Nishimura, Y., Turner, D. L., Glassmeier, K.-H., et al. (2012). Observations of a Pc5 global (cavity/waveguide) mode outside the plasmasphere by THEMIS. *Journal of Geophysical Research*, *117*(A6), A06202. https://doi.org/10.1029/2011JA017266

Kepko, L., Sibeck, D., Nakamura, R., Wiltberger, M., Merkin, V., Walsh, B., et al. (2022). Magnetospheric constellation: A key to unlocking the cross-scale coupling in the magnetosphere. In *44th cospar scientific assembly* (Vol. 44, p. 1605).

Kepko, L., Spence, H. E., & Singer, H. J. (2002). ULF waves in the solar wind as direct drivers of magnetospheric pulsations. *Geophysical Research Letters*, *29*(8), 1197. https://doi.org/10.1029/2001GL014405

Lepping, R. P., Acũna, M. H., Burlaga, L. F., Farrell, W. M., Slavin, J. A., Schatten, K. H., et al. (1995). The WIND magnetic field investigation. *Space Science Reviews*, *71*(1–4), 207–229. https://doi.org/10.1007/bf00751330

Li, S.-S., Angelopoulos, V., Runov, A., Kiehas, S. A., & Zhou, X.-Z. (2013). Plasmoid growth and expulsion revealed by two-point ARTEMIS observations. *Journal of Geophysical Research: Space Physics*, *118*(5), 2133–2144. https://doi.org/10.1002/jgra.50105

Liuzzo, L., Poppe, A. R., Halekas, J. S., Simon, S., & Cao, X. (2021). Investigating the Moon's interaction with the terrestrial magnetotail lobe plasma. *Geophysical Research Letters*, *48*(9), e93566. https://doi.org/10.1029/2021GL093566

Mann, I. R., Wright, A. N., Mills, K. J., & Nakariakov, V. M. (1999). Excitation of magnetospheric waveguide modes by magnetosheath flows. *Journal of Geophysical Research*, *104*(A1), 333–353. https://doi.org/10.1029/1998JA900026

Mathie, R. A., & Mann, I. R. (2000). Observations of an anomalously low frequency Alfvén continuum in an abnormally expanded magnetosphere. *Geophysical Research Letters*, *27*(24), 4017–4020. https://doi.org/10.1029/2000GL003791

McFadden, J. P., Carlson, C. W., Larson, D., Ludlam, M., Abiad, R., Elliott, B., et al. (2008). The THEMIS ESA plasma instrument and in-flight calibration. *Space Science Reviews*, *141*(1–4), 277–302. https://doi.org/10.1007/s11214-008-9440-2

Ness, N. F., Behannon, K. W., Scearce, C. S., & Cantarano, S. C. (1967). Early results from the magnetic field experiment on lunar Explorer 35. *Journal of Geophysical Research*, *72*(23), 5769–5778. https://doi.org/10.1029/JZ072i023p05769

Nykyri, K. (2024). Data set in CDF format [Dataset]. *Figshare*. https://doi.org/10.6084/m9.figshare.26384425.v1

Nykyri, K., Bengtson, M., Angelopoulos, V., Nishimura, Y., & Wing, S. (2019). Can enhanced flux loading by high-speed jets lead to a substorm? Multipoint detection of the christmas day substorm onset at 08:17 UT, 2015. *Journal of Geophysical Research: Space Physics*, *124*(6), 4314–4340. https://doi.org/10.1029/2018JA026357

Ogilvie, K. W., Chornay, D. J., Fritzenreiter, R. J., Hunsaker, F., Keller, J., Lobell, J., et al. (1995). SWE, a comprehensive plasma instrument for the WIND spacecraft. *Space Science Reviews*, *71*(1–4), 55–77. https://doi.org/10.1007/bf00751326

Plaschke, F., Glassmeier, K.-H., Auster, H. U., Constantinescu, O. D., Magnes, W., Angelopoulos, V., et al. (2009). Standing Alfvén waves at the magnetopause. *Geophysical Research Letters*, *36*(2), 2104. https://doi.org/10.1029/2008GL036411

Poppe, A. R., Samad, R., Halekas, J. S., Sarantos, M., Delory, G. T., Farrell, W. M., et al. (2012). ARTEMIS observations of lunar pick-up ions in the terrestrial magnetotail lobes. *Geophysical Research Letters*, *39*(17), L17104. https://doi.org/10.1029/2012GL052909

Rae, I. J., Mann, I. R., Murphy, K. R., Ozeke, L. G., Milling, D. K., Chan, A. A., et al. (2012). Ground-based magnetometer determination of in situ Pc4-5 ULF electric field wave spectra as a function of solar wind speed. *Journal of Geophysical Research*, *117*(A4), A04221. https://doi.org/10.1029/2011JA017335

Retinò, A., Khotyaintsev, Y., Le Contel, O., Marcucci, M. F., Plaschke, F., Vaivads, A., et al. (2022). Particle energization in space plasmas: Towards a multi-point, multi-scale plasma observatory. *Experimental Astronomy*, *54*(2–3), 427–471. https://doi.org/10.1007/s10686-021-09797-7

Samson, J. C., Greenwald, R. A., Ruohoniemi, J. M., Hughes, T. J., & Wallis, D. D. (1991). Magnetometer and radar observations of magnetohydrodynamic cavity modes in the Earth's magnetosphere. *Canadian Journal of Physics*, *69*(8–9), 929–937. https://doi.org/10.1139/p91-147

Samson, J. C., Harrold, B. G., Ruohoniemi, J. M., Greenwald, R. A., & Walker, A. D. M. (1992). Field line resonances associated with MHD waveguides in the magnetosphere. *Geophysical Research Letters*, *19*(5), 441–444. https://doi.org/10.1029/92GL00116

Samson, J. C., Wallis, D. D., Hughes, T. J., Creutzberg, F., Ruohoniemi, J. M., & Greenwald, R. A. (1992). Substorm intensifications and field line resonances in the nightside magnetosphere. *Journal of Geophysical Research*, *97*(A6), 8495–8518. https://doi.org/10.1029/91JA03156

Sarantos, M., Killen, R. M., Sharma, A. S., & Slavin, J. A. (2008). Influence of plasma ions on source rates for the lunar exosphere during passage through the Earth's magnetosphere. *Geophysical Research Letters*, *35*(4), L04105. https://doi.org/10.1029/2007GL032310

Simon, S., Kriegel, H., Saur, J., Wennmacher, A., Neubauer, F. M., Roussos, E., et al. (2012). Analysis of Cassini magnetic field observations over the poles of Rhea. *Journal of Geophysical Research*, *117*(A7), A07211. https://doi.org/10.1029/2012JA017747

Smith, J. M., Roberts, B., & Oliver, R. (1997). Magnetoacoustic wave propagation in current sheets. *Astronomy and Astrophysics*, *327*, 377–387.

Spreiter, J. R., Summers, A. L., & Rizzi, A. W. (1970). Solar wind flow past nonmagnetic planets—Venus and Mars. *Planetary and Space Science*, *18*(9), 1281–1299. https://doi.org/10.1016/0032-0633(70)90139-X

Stubbs, T. J., Halekas, J. S., Farrell, W. M., & Vondrak, R. R. (2007). Lunar surface charging: A global perspective using lunar prospector data. *Dust in Planetary Systems*, *643*, 181–184.

Sugiura, M., & Wilson, C. R. (1964). Oscillation of the geomagnetic field lines and associated magnetic perturbations at conjugate points. *Journal of Geophysical Research*, *69*(7), 1211–1216. https://doi.org/10.1029/JZ069i007p01211

Tanaka, T., Saito, Y., Yokota, S., Asamura, K., Nishino, M. N., Tsunakawa, H., et al. (2009). First in situ observation of the Moon-originating ions in the Earth's Magnetosphere by MAP-PACE on SELENE (KAGUYA). *Geophysical Research Letters*, *36*(22), L22106. https://doi.org/10.1029/2009GL040682

Tóth, G., Sokolov, I. V., Gombosi, T. I., Chesney, D. R., Clauer, C. R., De Zeeuw, D. L., et al. (2005). Space weather modeling framework: A new tool for the space science community. *Journal of Geophysical Research*, *110*(A12), A12226. https://doi.org/10.1029/2005JA011126

Tsyganenko, N. A. (1996). Effects of the solar wind conditions on the global magnetospheric configuration as deduced from data-based field models. In *Proceedings of the ICS-3 conference on substorms (Versailles, France May 12–17, 1996)* (pp. 181–185).

Viall, N. M., Kepko, L., & Spence, H. E. (2009). Relative occurrence rates and connection of discrete frequency oscillations in the solar wind density and dayside magnetosphere. *Journal of Geophysical Research*, *114*(A1), 1201. https://doi.org/10.1029/2008ja013334

Villante, U., Francia, P., & Lepidi, S. (2001). Pc5 geomagnetic field fluctuations at discrete frequencies at a low latitude station. *Annales Geophysicae*, *19*(3), 321–325. https://doi.org/10.5194/angeo-19-321-2001

Whang, Y. C. (1970). Two-dimensional guiding-center model of the solar wind-Moon interaction. *Solar Physics*, *14*(2), 489–502. https://doi.org/10.1007/BF00221333

Wieser, M., Barabash, S., Futaana, Y., Holmström, M., Bhardwaj, A., Sridharan, R., et al. (2010). First observation of a mini-magnetosphere above a lunar magnetic anomaly using energetic neutral atoms. *Geophysical Research Letters*, *37*(5), 5103. https://doi.org/10.1029/2009GL041721

Wilson, J. K., Mendillo, M., & Spence, H. E. (2006). Magnetospheric influence on the Moon's exosphere. *Journal of Geophysical Research*, *111*(A7), 7207. https://doi.org/10.1029/2005JA011364

Zhang, H., Khurana, K. K., Kivelson, M. G., Angelopoulos, V., Wan, W. X., Liu, L. B., et al. (2014). Three-dimensional lunar wake reconstructed from ARTEMIS data. *Journal of Geophysical Research: Space Physics*, *119*(7), 5220–5243. https://doi.org/10.1002/2014JA020111